PHYSICAL REVIEW D
PARTICLES AND FIELDS

THIRD SERIES, VOLUME 29, NUMBER 5 1 MARCH 1984

Cryogenic search for fractionally charged particles

W. Kutschera, J. P. Schiffer, D. Frekers, W. Henning, M. Paul,* and K. W. Shepard
Argonne National Laboratory, Argonne, Illinois 60439

C. D. Curtis and C. W. Schmidt
Fermi National Accelerator Laboratory, Batavia, Illinois 60510
(Received 28 July 1983)

An experiment was performed to test the hypothesis of cryogenic trapping of fractionally charged particles, suggested as a possible explanation for the results of LaRue, Fairbank, Hebard, and Phillips at Stanford. A Nb-filament source was built, which could be cooled to 4.2 °K and rapidly heated to several hundred °K. The source was operated in the terminal of a 700-kV Cockcroft-Walton accelerator and energy spectra of positively charged particles emerging from the filament were measured under a variety of operating conditions. No events above a background of 10^{-2} counts/sec were found in the energy regions where one might have expected several hundred particles of charge $+\frac{1}{3}e$ or $+\frac{2}{3}e$ as the source was heated. A mass range from 10 MeV/c^2 to 100 GeV/c^2 was covered in the experiment. Although negative results are rarely unambiguous, our findings exclude one class of hypotheses which might have explained the apparent fractional charges of the Stanford experiments.

I. INTRODUCTION

The question of the existence of stable free fractional charges has been of considerable experimental interest since the emergence of quark models two decades ago. Numerous experiments were performed, none of which showed conclusive evidence for fractional charges with limits of concentrations (depending on assumptions and methods) of 10^{-12}–10^{-30} fractional charges per nucleon.[1] Since 1977, however, the group at Stanford[2] has been reporting positive results from measurements that involve the levitation of superconducting Nb spheres in a magnetic field. A conceivable hypothesis was discussed by one of us,[3] that the low temperatures used in the Stanford experiment may play a special role in trapping fractional charges. It is perhaps not unreasonable to postulate that $(+\frac{1}{3}e)$ particles, because they bind electrons so weakly, would be extremely mobile and diffuse rapidly through most materials at room temperature, but may be frozen in place at cryogenic temperatures—much as hydrogen diffuses readily through many metals above ~ 1000 °K, yet is effectively frozen in place at room temperature. This mobility might then be related to the apparent ease with which fractional charges seemed to change on Nb spheres in the Stanford experiment.[2] Possibly even $(+\frac{2}{3}e)$ particles might behave in such a fashion.

In order to test this hypothesis one may cool a piece of Nb metal to a low temperature, similar to the temperatures in the Stanford experiment, and let it remain cold for some time in order to allow for the hypothetical $(+\frac{1}{3}e)$ particles to be frozen out from some ambient concentration. (There is no obvious reason for taking Nb metal, except that this material has been used in the Stanford experiment.) One may estimate[4] that in order to have a reasonable probability of trapping such particles in the Stanford experiment, the ambient concentration for a gas of $(+\frac{1}{3}e)$ particles would have to be at least $\sim 1/\mathrm{m}^3$. If the Nb metal were in the terminal of an electrostatic machine which is now raised to a positive voltage V, and the filament is suddenly heated to 300 °K or higher, then any positively charged particle of charge q that is released from the Nb surface will be accelerated to an energy qV. If there are no magnetic fields, in other words if all the focusing and steering is done electrostatically, then all particles will converge to the same focus, independent of their charge or mass. Since heating the filament is a matter of a fraction of a second, one should be able to detect even a single particle with energy $\frac{1}{3}$ eV, if background rates are ≤ 1/sec. The energy measurement is best carried out with a detector that measures the total kinetic energy with good resolution, a solid-state detector is particularly well suited for this purpose. Using the Stanford experiments as a guide, the probability of trapping a fractional charge on a Nb sphere of 140 μm radius would be

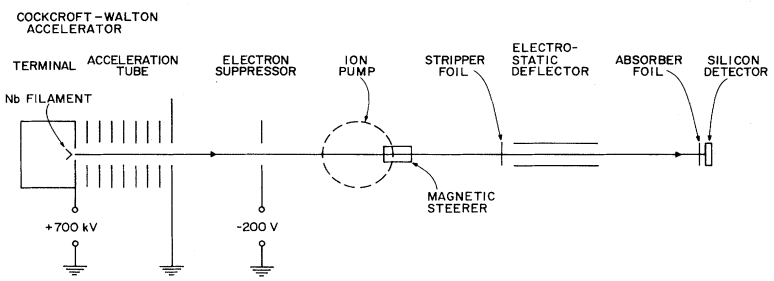

FIG. 1. Schematic layout of the experiment to detect $(+\frac{1}{3}e)$ particles emerging from a Nb filament. With the electrostatic deflector on, the particle detector was moved to the appropriate off-zero position. The magnetic steerer was only used in setting limits for light particles, with less than $\frac{1}{10}$ of the proton mass (see Sec. III C).

$\sim 30\%$ and a Nb surface of ~ 40 mm^2 would trap on the order of ~ 50 such particles. If volume effects are important this number might increase to several hundred particles.

The requirements of a cryogenic system in the terminal of a high-voltage machine are for considerable space and, if practical, atmospheric pressure. Both of these requirements are available in Cockcroft-Walton accelerators frequently used as injectors of large accelerator complexes.

II. EXPERIMENTAL SETUP

The experiment was performed at the Fermi National Accelerator Laboratory using one of the Cockcroft-Walton injectors. The terminal of these injectors is usually operated at a negative potential of 750 kV, providing H^- ions suitable for the subsequent high-energy acceleration system. During the shut-down period of the main accelerator ring for installation of superconducting magnets one of the two injectors was made available for our experiment. The polarity was reversed since we were interested in searching for $(+\frac{1}{3}e)$ particles. Fortunately our injector had a zero degree exit port through a bending magnet, which allowed us to install a short beam line with a small scattering chamber. Figure 1 shows in a schematic way the essential components of the experimental setup. In normal operation of the injector several magnetic elements (not shown in Fig. 1, except for one magnetic steerer) are used to focus the intense H^- beam. For our experiment these elements were carefully degaussed in order to minimize the deflections of possible low-mass particles by the residual magnetic field. The remaining system was essentially purely electrostatic, hence delivering any positive particle, independent of its charge and mass, from the Nb filament to the particle detector. However, in order to reduce the background from unwanted particles, such as hydrogen clusters and possible heavy atoms, a combination of a 10-μg/cm^2 carbon stripper foil, an electrostatic deflector, and a 100-μg/cm^2-thick aluminum absorber foil were placed in front of the particle detector.

Acceleration of positively charged particles was provided by the Cockcroft-Walton accelerator. After conditioning to 750 kV the accelerator could usually be operated stably at 700 kV. During data-taking runs the fluctuations of the voltage were well below 1%. Occasional small changes were easily detected since the voltage was continuously monitored. A spark, of course, always gave a very clear signature. The vacuum in the system was supplied by a 2400-liter/sec magnetic ion pump. Backstreaming electrons from this pump, accelerated toward the terminal, produced a considerable number of background ions. A suppressor ring at -200 V (see Fig. 1) reduced this background by a factor of 10. With the source at room temperature the pressure was in the low 10^{-7}-Torr range and with the source cold about 5×10^{-8} Torr.

The heart of the experimental setup was a cryogenic ion source built specifically for the present investigation. Figure 2 shows some details of the source and the ion-optical elements. This arrangement allowed rapid control of the temperature of a Nb filament over a range $4.2 \leq T \leq 1200$ °K and transported any positive particle emerging from the tip of the filament to the particle detector. The tip was 3 mm wide$\times$5 mm long$\times$1 mm thick, which formed a surface area of 40 mm^2 and a volume of 15 mm^3. A series of measurements described in Sec. III A ensured that the extraction and acceleration optics produced an image of the filament tip well within the size of the particle detector. The Nb filament was formed from 1-mm-thick Nb metal sheet bonded (explosively) on both ends to thick copper bars which provided a thermal path to liquid helium. The filament could be driven from $T=4.2$ °K to $T>300$ °K in less than 1 sec by inducing several hundred amperes of 60-Hz current with the transformer located in the helium bath. The temperature was controlled by adjusting the ac voltage drop across the filament. The voltage drop had been previously calibrated against temperature by direct measurement with a copper-constantan thermocouple attached to the filament tip for $T<650$ °K, and with an optical pyrometer for $T\leq 1400$ °K. In addition, the current through the filament was measured with a pickup coil, which provided a particularly clear signal for the transition from superconducting (high-current) to normal (low-current) state. A continuous flow of liquid nitrogen (LN_2) and liquid helium from 100-liter storage Dewars located in the high-voltage terminal supplied the necessary cooling. It was possible to change the liquid-helium storage Dewar without substantial loss of liquid in the filament cryostat, so that the Nb filament could be kept cold for extended

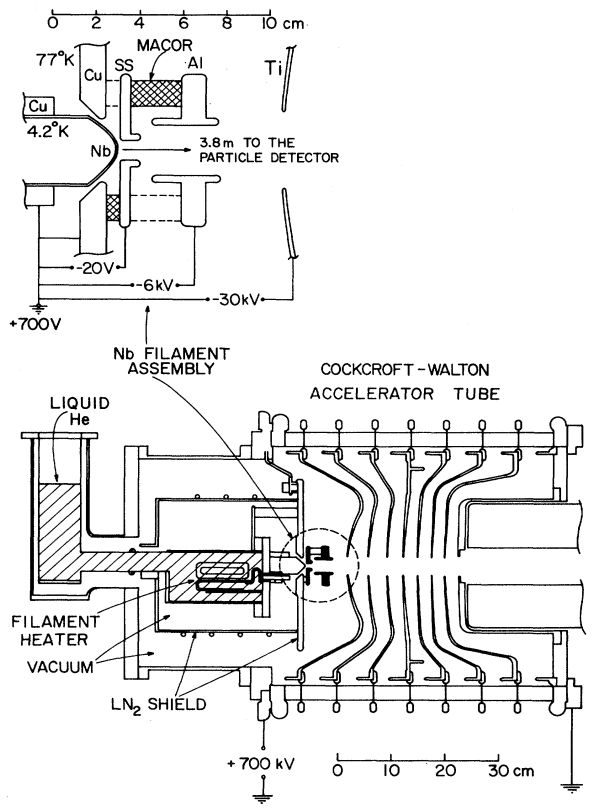

FIG. 2. Simplified layout of the cryogenic source and the acceleration structure. The cold part of the source was held in place by three stainless-steel brackets which restricted the Nb filament motion during cool-down to less than 0.1 mm. The top insert shows details of the Nb filament assembly and the extraction geometry. Materials used are indicated (SS = stainless steel, Macor = machinable glass-ceramic insulator).

periods of time (typically 10 h with two Dewars).

The particle energy was measured with a 300- or 2000-μm-thick Si surface-barrier detector (area = 100 mm^2) located at a distance of 3.8 m from the Nb filament. An energy measurement by ionization sets an upper limit for an observable mass, since below a certain velocity not all the energy will produce a detectable signal. For "normal" particles this domain can be estimated from the Lindhard-Scharff-Schiøtt (LSS) theory.[5] This description is not directly applicable to $+\frac{1}{3}e$ particles, since they cannot screen their charge in the same way as integrally charged particles, but it may not be unreasonable to assume that at low velocities the fractionally charged particles have at least the ionizing strength of normal particles. As a guide for an upper mass limit we have therefore estimated with the LSS description the mass of $Z=1$, 233-keV particles for which the nuclear stopping-power contribution is small compared to the electronic part. This results in an approximate upper mass limit of 100 GeV/c^2. The lower mass limit is determined by the deflection of light particles in residual magnetic fields along the flight path. As shown in the next section, hydrogen clusters of different mass could be used to estimate the integral residual-field effect. This field was then compensated by a small magnetic steering field (cf. Fig. 1) for searches of light particles setting a lower mass limit of 10 MeV/c^2.

III. MEASUREMENTS AND RESULTS

A. Initial tests

An important part of the experiment was the testing of the ion optics to guarantee an efficient collection of positively charged particles from the Nb filament. For these measurements the Nb filament was first replaced by a 5-mm-diameter lithium surface-ionization pellet[6] which easily gave a Li^+ current of a few hundred nA. An immersion-lens geometry frequently used in mass spectrometers was chosen as an efficient and ion-optically flexible extraction system. It consisted of two cylindrical lenses shown in Fig. 2 and provided a suitable matching to the optics of the accelerator tube. With the accelerator at 700 kV the best imaging conditions were found with -20 V on the first and -6 kV on the second electrode. With these potentials a 2-mm-diameter beam spot was formed on a quartz plate close to the detector position. Once the alignment of the system was established with the Li^+ beam the Nb filament was mounted and the alignment checked by heating it to about 900 °C. At this temperature the filament emitted enough positive ions to see a faint beam spot on a ZnS(Ag) screen. With this condition the spot had a diameter of approximately 3 mm.

The next step was the reduction of background particles in the energy region of interest. Figure 3 shows a series of energy spectra which indicate a variety of different background conditions. In these figures the counting rate in 3.9-keV energy bins is plotted as a function of the particle energy. In Fig. 3(a) the source was cooled only with liquid nitrogen and all particles accelerated were measured in the Si detector. A full-energy peak (mainly H^+ ions) at 700 keV is clearly seen. At lower energies a large continuous bump of perhaps heavier particles originating from somewhere in the acceleration tube are seen. Part of this bump could be absorbed by a 100-μg/cm^2-thick Al foil in front of the detector [Fig. 3(b)]. A 300-μm detector with better energy resolution than in Fig. 3(a) was used for the measurements of Figs. 3(b)—3(e). The Al foil also separates H_2^+ particles from H^+, since the former lose more energy. In a first approximation the energy loss of a molecule is the sum of the energy losses of its constituents. However, for foil-crossing times short compared to that needed to significantly separate the "Coulomb-exploding" constituents, the energy loss can be higher (e.g., H_2 behaves more like a ^{2}He particle). When the Nb filament was cooled to 4.2 °K, H_3^+ molecules showed up [Fig. 3(c)]. These clusters are particularly dangerous since breakup products can easily mimic the energy of a $(+\frac{1}{3}e)$ particle (e.g., H^+ particles originating from the breakup of H_3^+). In order to remove these clusters a 10-μg/cm^2-thick carbon stripper foil and an electrostatic deflector were installed (cf. Fig. 1). With the stripper foil in and the deflector off, a variety of breakup products are seen in the energy spectrum of Fig.

3(d). In Fig. 3(e) a voltage of 5 kV was put on the deflector (plate length 15 cm, plate separation 1.5 cm, distance to the detector 29 cm) and the detector moved to a position of maximum H^+ yield. This displacement was 14 mm, and all the ions whose charge and mass remained unchanged in the stripper foil, had to be deflected by the same amount. Since the various breakup products did not match this condition they were very efficiently removed. The spectra of Figs. 3(a) through 3(e) were measured without the −200-V on the suppressor ring, so that the filament was bombarded by electrons from the ion pump. The dashed H^+ peak in Fig. 3(e) indicates that the counting rate (in the whole energy range) was reduced by a factor of 10 when the suppressor was on. This then brought the counting rate down to $\lesssim 0.1$ counts/min in the interesting energy region comparable to the background of the detector by itself, isolated from the accelerator [Fig. 3(f)].

B. Data recording

The procedure to search for $(+\frac{1}{3}e)$ particles was as follows: First the Nb filament was cooled to 4.2 °K and kept cold with the extraction and accelerating voltages turned off. After a period of several hours the data taking was started. In order to accurately trace the operating conditions of the system a number of parameters were monitored as a function of time. At the terminal, the analog signals of the temperature of the LN_2 shield, of the current and voltage (determining the temperature) of the Nb filament, and of the two extraction voltages were digitized and transmitted via microprocessor and light link with a repetition rate of 15 Hz to a PDP 11/45 computer. In the same way, the acceleration voltage and the vacuum reading were transmitted from ground potential. These data were reconverted into analog signals and read via CAMAC analog-to-digital converters (ADC's) into the computer memory, whenever a 60-Hz pulser or a detected event provided a look-at-me LAM signal. The pulser also served as a monitor for the stability and resolution of the detection system. In addition a time spectrum was generated with a 1- or 5-Hz pulser fed into a scaler which was read out whenever the LAM signal was present. All signals were recorded event by event on magnetic tape providing a detailed history of each run.

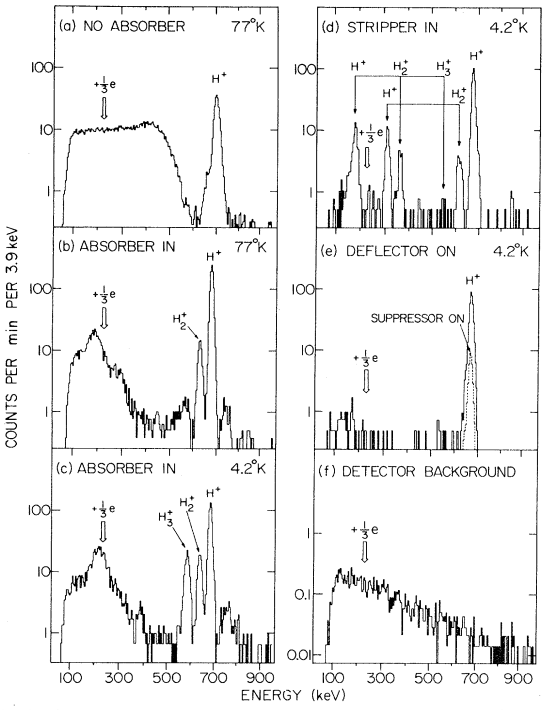

FIG. 3. Energy spectra measured in the Si surface-barrier detector. The various operating conditions are described in the text. The arrows indicate the approximate position of particles with charge $+\frac{1}{3}e$. The actual energy of these particles measured in the detector might be slightly lower than indicated in spectra (b) to (e) due to the energy loss in the Al absorber (see Sec. III C). The detector background (f) was measured with a 2000-μm detector. It was a factor of 3 lower for a 300-μm detector [see Fig. 18(b)].

C. Search runs

1. *Run A*

Figure 4 shows a spectrum of the cold Nb filament after the first long He cooling period of 9.5 h. The trace of the full-energy peak (H^+) is clearly visible. The energy loss in the stripper and absorber foils of the H^+ particles was about 30 keV. In Fig. 5 the time distribution of events in the H^+ peak and in two regions where one might expect $(+\frac{1}{3}e)$ and $(+\frac{2}{3}e)$ particles is shown. In this and subsequent figures the energy regions for possible fractional charges were chosen by assuming protons of the corresponding energies and multiplying the energy loss by $(\frac{1}{3})^2$ and $(\frac{2}{3})^2$, respectively. For all energy windows the full width of the H^+ peak was used (40 keV). The counting rate of H^+ particles with the filament cold was about 40 counts/min. It is apparent from Figs. 4 and 5 that the background in the regions of interest is extremely low. Figures 6 and 7 show the history of the first heating.

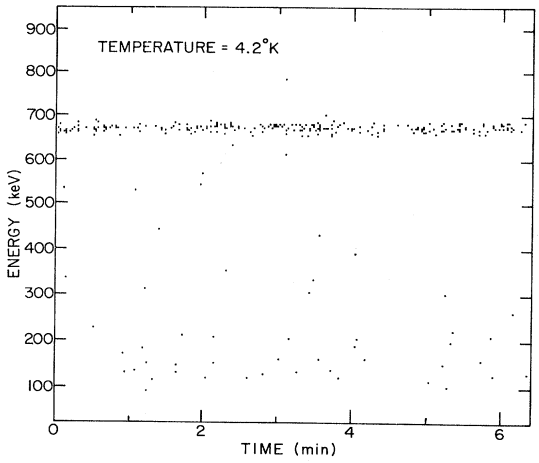

FIG. 4. Two-dimensional display of the events measured in a 300-μm Si detector as a function of time in run A, after a He cooling period of 9.5 h. The event threshold allows for single counts to be visible.

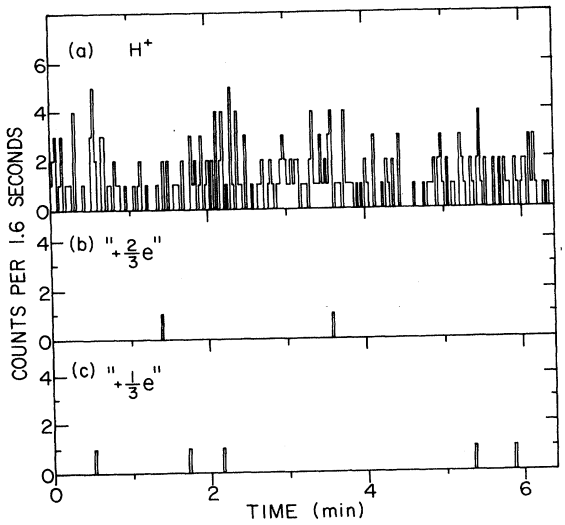

FIG. 5. Time distribution of events in three energy windows set on the spectrum of Fig. 4 (run A) at the position of the H^+ peak (650–690 keV) and at two regions where one might expect $+\frac{1}{3}e$ (206–246 keV) and $+\frac{2}{3}e$ (428–468 keV) particles. The time resolution of the data recording was 0.2 sec, compressed by a factor of 8 in this figure.

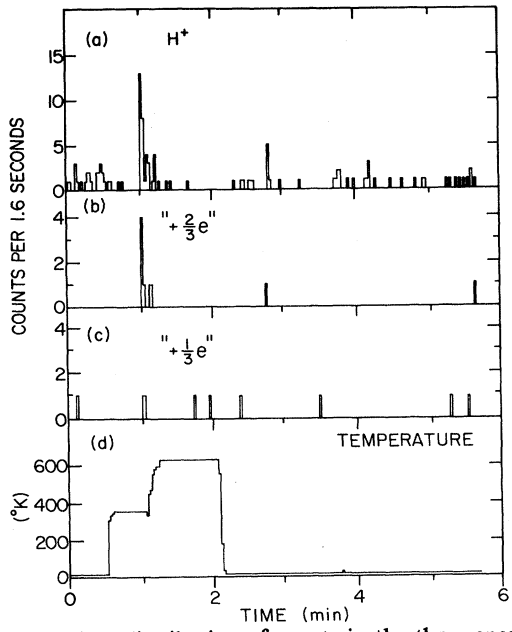

FIG. 7. Time distribution of events in the three energy windows set on the spectrum of Fig. 6, from run A. The energy intervals for the windows are those of Fig. 5.

These data were taken immediately after the previous one. At the bottom of Figs. 6 and 7 the temperature of the Nb filament is displayed. (In these and subsequent figures the lowest temperature corresponds to a superconducting condition.) The first heating to about 350°K reduced the H^+ counting rate, an effect which was always observed when the filament was warmed up. This indicates that the origin of the H^+ particles is hydrogen condensed onto the cold filament, apparently being depleted when the temperature is raised. At the 1-min mark a spark occurred accompanied by a burst of particles seen in Figs. 6 and 7. After the temperature had risen to 620°K a broad low-energy bump appeared (Fig. 6). Figure 8 shows the energy spectrum of this time period. Both Figs. 7 and 8 show no significant events in the interesting energy regions. In a somewhat longer second run with heating during the same cool-down period the temperature was raised to 260 and 480°K (Figs. 9 and 10), with no excess particles showing up. The depletion of hydrogen during the heating is more clearly seen in these runs because of a compressed time scale.

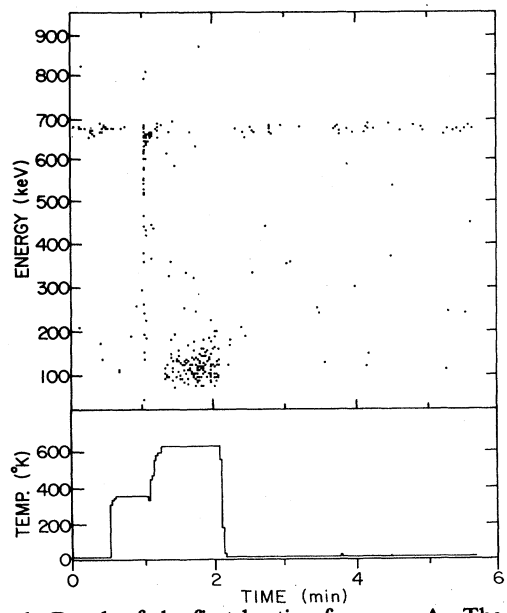

FIG. 6. Result of the first heating from run A. The bottom spectrum gives the temperature profile of the filament. The burst of particles at the 1-min mark was caused by a spark.

2. *Run B*

Next we changed the detection system by removing the 100-μg/cm^2 Al absorber foil. Otherwise the experiment

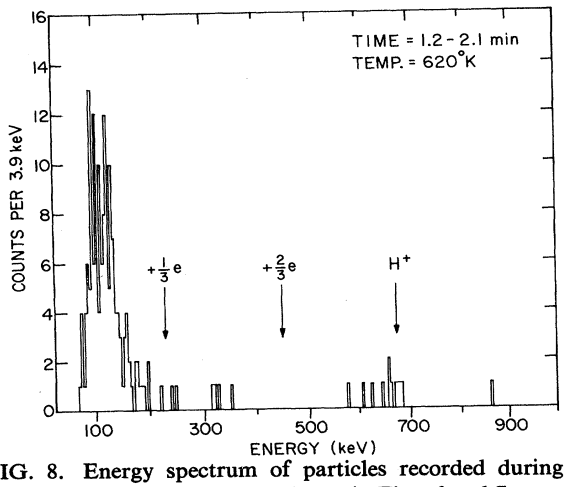

FIG. 8. Energy spectrum of particles recorded during the highest heating period of run A shown in Figs. 6 and 7.

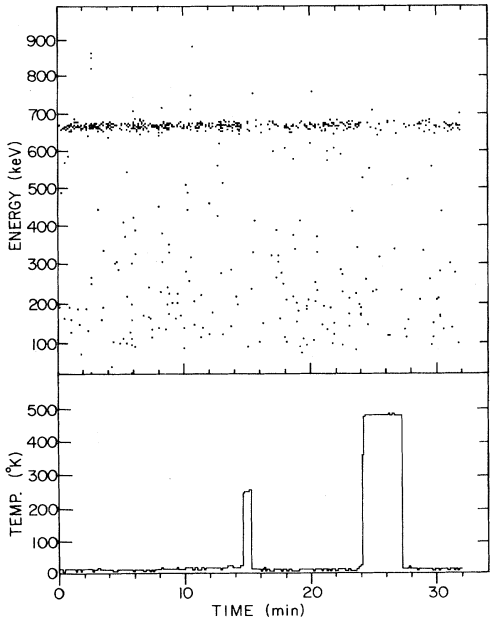

FIG. 9. Result of the second heating from run A with a time scale compressed by a factor 5 as compared to the spectra of Figs. 4 to 7.

stayed the same, with the carbon stripper in and the deflector on. This was done on the remote chance that the particles we were looking for had an anomalously large energy loss. After a He cooling period of 7.5 h data taking was started with the extraction and acceleration voltage off (Fig. 11) for 6 min, then the voltages were switched on and the trace of the H^+ peak appeared. Figure 12 shows the time distribution of the energy windows,

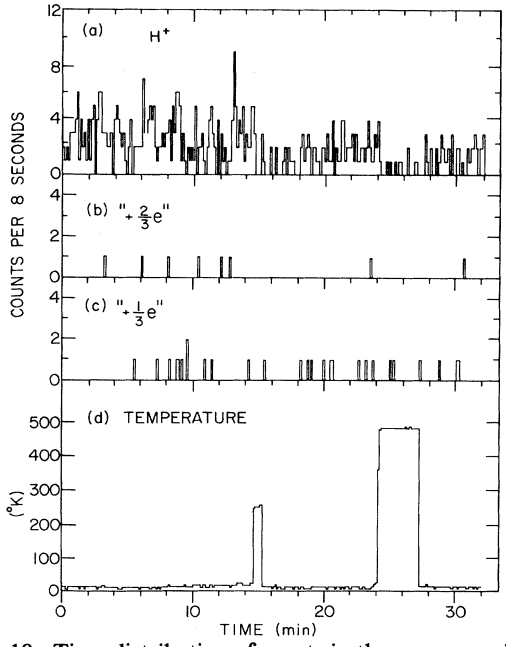

FIG. 10. Time distribution of events in three energy windows set on the spectrum of Fig. 9, from the second heating in run A. The energy intervals of the windows are those of Fig. 5.

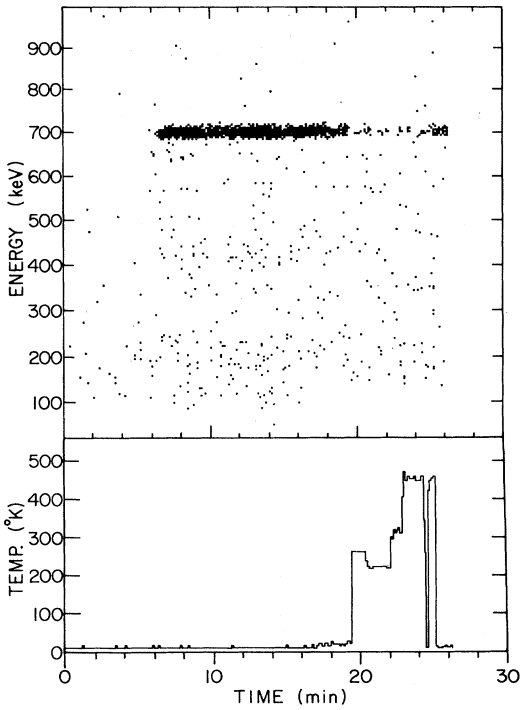

FIG. 11. Result of the first heating from run B after a He cooling period of 7.5 h, with the Al absorber removed. Data taking was started with all voltages off. They were switched on at the 6-min mark.

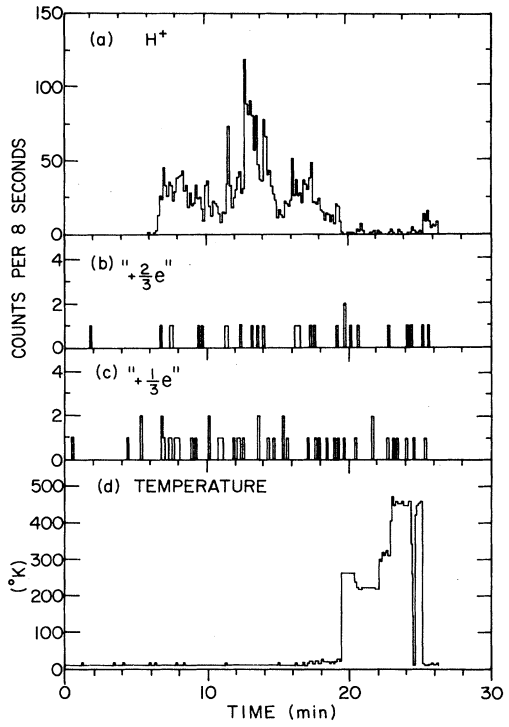

FIG. 12. Time distribution of events from run B in three energy windows set on the spectrum of Fig. 11. The energies were 676–716 keV for the H^+ peak, 446–486 keV for the "$+\frac{2}{3}e$" windows, and 212–252 keV for the "$+\frac{1}{3}e$" window.

set at somewhat higher energies as compared to the previous runs, since the Al absorber foil was out. (The counting rate of H^+ was higher and less uniform with time as compared to the previous runs, probably due to a somewhat worse vacuum condition.) During the heating the H^+ peak is clearly depleted and no excess counts show up in the "fractional-charge" windows. Figures 13 to 15 show the result of a second run with heating to higher temperatures. At 620°K a broad peak around 400 keV appeared, likely to be of the same origin as the low-energy tail observed when the Al absorber was used (Figs. 6 to 8). This peak disappeared when the temperature was lowered below 600°K. The peaks in the fractional-charge energy windows of Fig. 14 are due to the long tails of the 400-keV peak (cf. Figs. 13 and 15). The origin of the broad peak is probably complex. The most likely candidates are heavy alkaline ions (e.g., K^+) which may have some probability for surface ionization above 600°K. The energy loss of 700-keV K^+ ions in the 10-μg/cm^2 carbon stripper foil and the 40-μg/cm^2 gold layer of the silicon detector is estimated[7] to be about 60 keV. The measured energy in Fig. 15 is considerably lower than 640 keV probably due to pulse-height defects in the detector. The very-low-energy signals observed with the 100-μg/cm^2 Al absorber in (Fig. 8) is then due to the additional energy loss of approximately 300 keV.[7] Molecular-breakup products (e.g., large hydrogen clusters from a complex carbohydrate molecule) could also result in the observed energies. However, most such products should be removed by the stripper-deflector system (cf. Fig. 3).

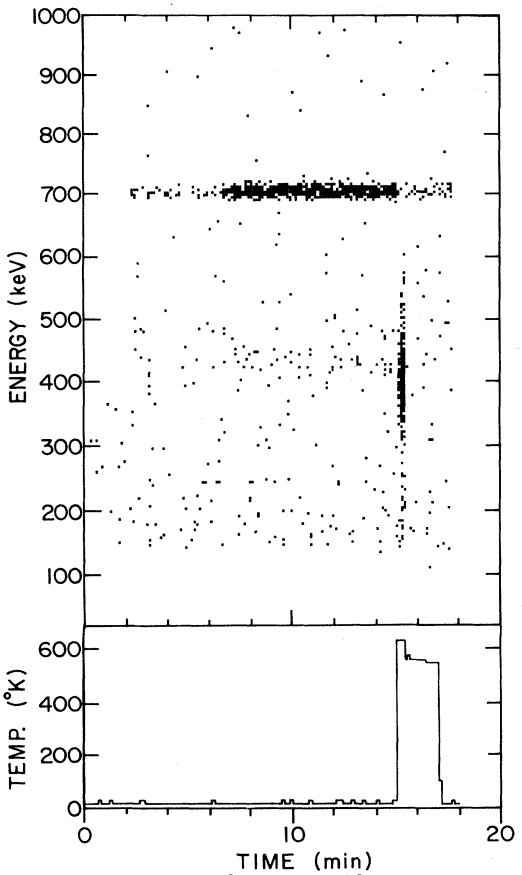

FIG. 13. Second heating from run B following that of Fig. 11. A broad peak shows up around 400 keV when the temperature reaches 620°K.

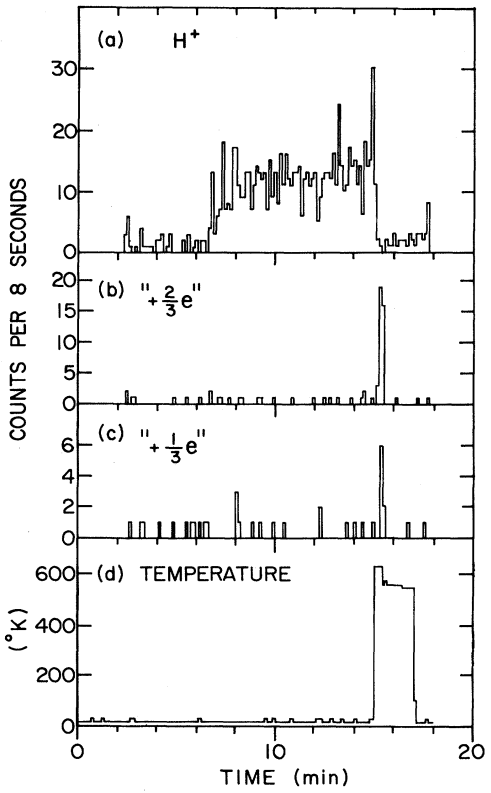

FIG. 14. Time distribution of events in three energy windows set on the spectrum of Fig. 13, from the second heating in run B. The energy intervals for the windows were the same as in Fig. 12.

3. *Run C*

Figures 16 and 17 show the result of another run without Al absorber after a He cooling period of 7.2 h. When the accelerator voltage was turned on a spark occurred releasing a burst of particles over the whole energy

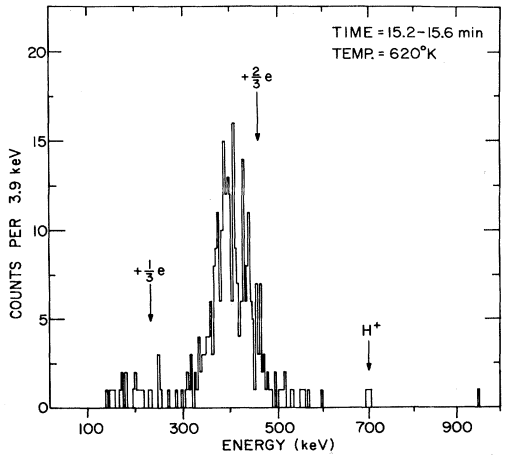

FIG. 15. Energy spectrum of particles recorded when the Nb filament was at 620°K (see Fig. 13) in run B.

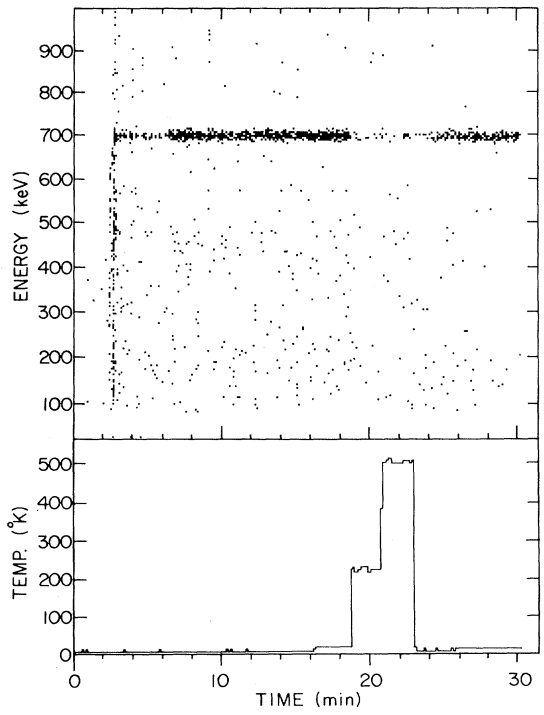

FIG. 16. Result of the first heating in run C after another He cooling of 7.2 h, with the Al absorber still out.

range. In the subsequent heating up to 500°K no excess events were observed.

4. Run D

Figure 18 shows the result of a very long run at He temperature with no heating and a 75-μg/cm^2 Al absorber in front of the detector. There are some minor peaks showing up in the energy spectrum, possibly remnants of the hydrogen-cluster breakups (cf. Fig. 3).

5. Run E (residual-magnetic-field compensation)

As mentioned in Sec. II, one might miss possible very light fractionally charged particles by their deflection in residual magnetic fields, including the Earth's magnetic field. We have measured the field distribution with a Hall probe both vertically and horizontally over the entire length of the particle flight path. Vertical fields varied from 0 to 0.5 G. Horizontal components were a factor 2 to 3 smaller. In order to compensate for the integral effect of the vertical component we measured the effect of small additional fields supplied by a magnetic steerer, located approximately half-way between the Nb filament and the particle detector (cf. Fig. 1). Since the deflection is mass dependent we used the different position shifts of the H^+, H_2^+, and H_3^+ peaks to find the best field setting. Figure 19 shows clearly the different response of H^+ and H_3^+ to the steerer fields. The optimum field was found by plotting the centroid position of the H^+, H_2^+, and H_3^+ peaks as a function of the steerer field (Fig. 20). From

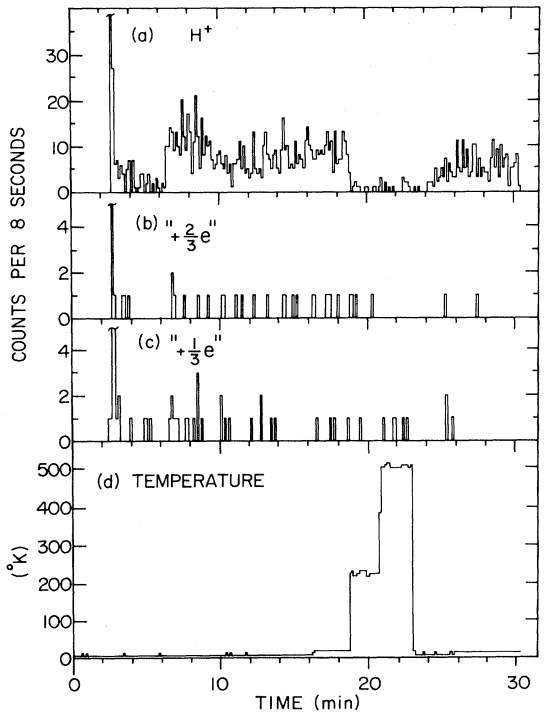

FIG. 17. Time distribution of events in three energy windows set on the spectrum of Fig. 16, for run C. The energy intervals for the windows were the same as in Fig. 12.

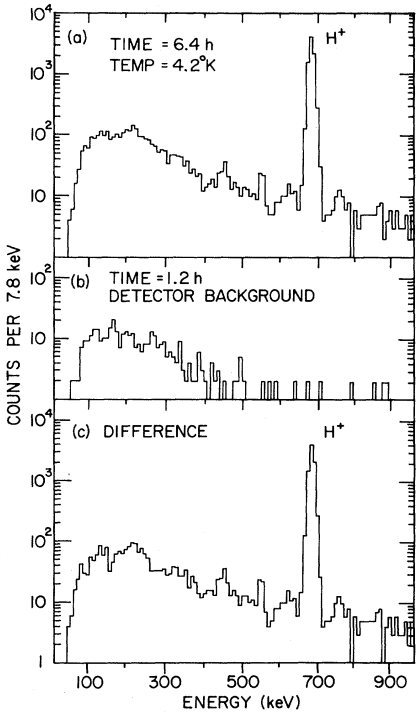

FIG. 18. Energy spectra of a long run (run D) with the Nb filament at He temperature. In spectrum (c) the normalized background of (b) has been subtracted from spectrum (a).

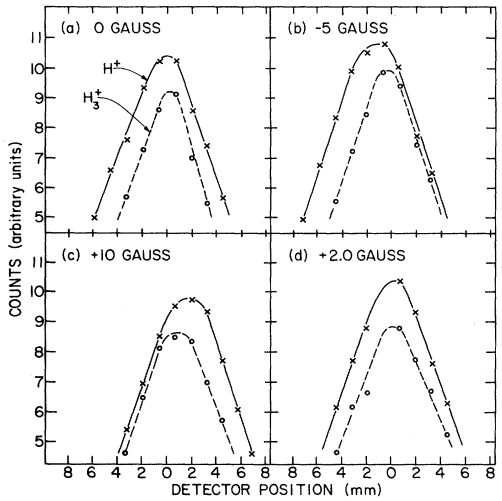

FIG. 19. Position shifts of the H^+ and H_3^+ peaks for various magnetic steerer field settings, measured by scanning the beam profile with the silicon detector (10 mm aperture). The setting of Fig. 19(d) was deduced from the plot of Fig. 20, showing essentially identical positions for both particles. The curves are "eye fits" to the data points.

this we chose a "zero-deflection" field of $+2.0$ G. With this field setting we estimated a reasonable acceptance for particles with masses ≥ 10 MeV/c^2.

Since lighter mass particles would have a longer range, we replaced the 300-μm thick Si detector with a-2000-μm one. In addition, a 4.8-mg/cm^2 thick Al absorber was mounted (instead of the 100-μg/cm^2 one) in front of the detector, which stopped all "normal" particles including protons. For these measurements the electrostatic deflector was off and the detector positioned at zero degrees exactly. Figures 21 and 22 show the result of a run with heating after a He cooling period of 9.7 h. It is obvious that we find no indication of an effect when the filament was heated to 800°K. The accelerator-independent background for the 2000-μm detector is higher than for the 300-μm one, due to its larger volume.

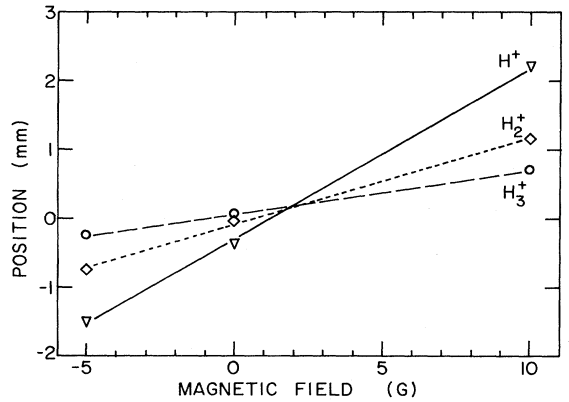

FIG. 20. Plot of the position of the centroids of the H^+, H_2^+, and H_3^+ peaks as a function of steering field. The different slopes meet at 2.0 G, which was chosen as the best setting for light-particle searches.

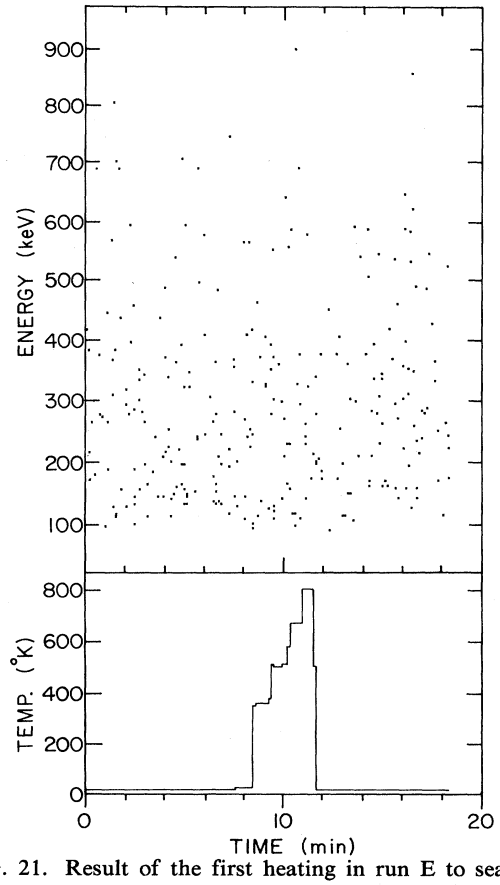

FIG. 21. Result of the first heating in run E to search for light particles, after a cooling period of 9.7 h. No H^+ particles are observed due to the thick Al absorber (4.8 mg/cm^2).

6. *Runs F and G (helium)*

As a remote possibility for trapping of fractionally charged particles we finally made a series of runs after bleeding He gas into the vacuum system, with the source cold. This gas was supplied from a liquid helium Dewar. Helium gas as the possible source for the fractional charges observed in the Stanford experiments[2] was conjectured by Boyd *et al.*,[8] since it was used[2] as a heat conductor in these[2] experiments. Helium gas from the Dewar was leaked into our vacuum system with all voltages off. By this procedure the pressure in the system was raised from 8×10^{-8} to 5×10^{-4} Torr for 1 hour. The ion pump was closed off during this period and the system pumped with a 100-liter/sec turbomolecular pump. From this condition one estimates a total supply of about 3×10^{22} He atoms to the system. Spectra measured after this procedure are shown in Figs. 23 to 25 (thin Al absorber) and in Figs. 26 and 27 (thick Al absorber and magnetic-field compensation). The only prominent particle group observed was the low-energy tail seen in previous runs (Figs. 6 to 8), when the temperature was raised to 620°K and with the 100-μg/cm^2 Al absorber in use.

The results from all the runs are summarized in Table I. The table lists the various parameters of the detection system and the number of counts in the regions of interest. The temperature is ordered chronologically and a

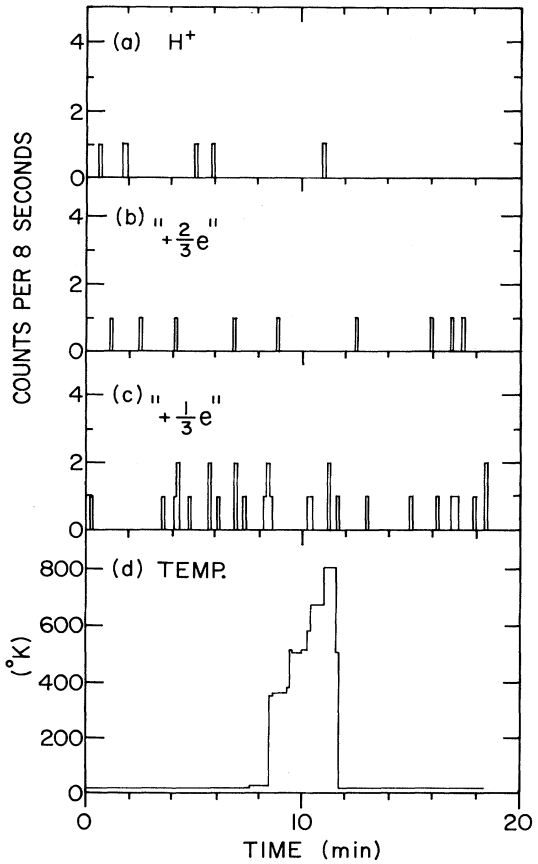

FIG. 22. Time distribution of events in three energy windows set on the spectrum of Fig. 21, from run E. The energy intervals for the windows were the same as in Fig. 12.

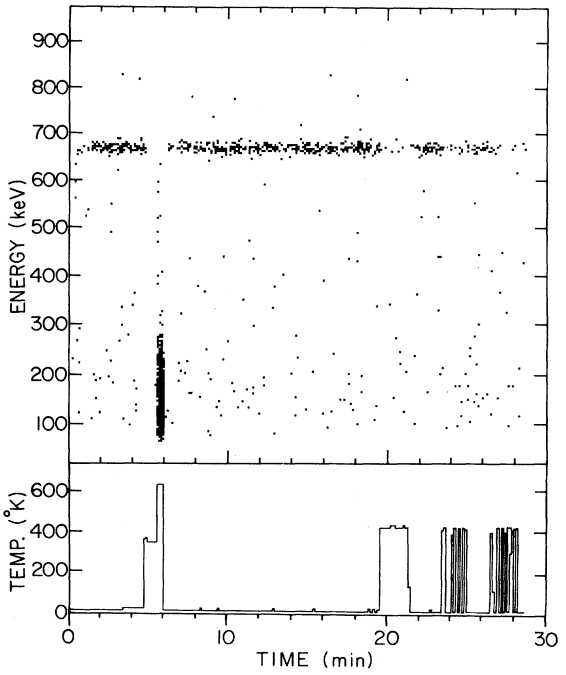

FIG. 23. First heating in run F after He was leaked into the system. A 100-μg/cm^2 Al absorber was used in this run. The strong low-energy tail at 620°K was also observed in previous runs (Figs. 6–8).

correspondence to the figures can easily be established.

IV. DISCUSSION

It is clear from our results that no excess events were observed in the first few seconds after the Nb metal was heated either to 300°K or to 500°K after it had been cooled for several hours. After this the events were randomly distributed in energy at a rate lower than, or at most equal to the background ($\sim 10^{-2}$ counts/sec) seen with the filament cold. The surface and volume of the Nb-filament tip used in our experiment was 40 mm^2 and 15 mm^3, respectively. The corresponding values for the Nb spheres ($r = 140$ μm) used in the Stanford experiment[2] are 0.25 mm^2 and 0.012 mm^3. From this it follows that in our experiment the Nb surface is a factor 160 and the volume a factor 1250 larger. Thus, the expected signal would have been of several hundred pulses at an energy of ~ 233 keV emitted shortly after heating. The result is clearly negative, the hypothesis of cryogenic trapping of $(+\frac{1}{3}e)$ charges as an explanation of the results of Ref. 2 does not seem to be supported.

There are of course, as is always the case with a negative result of this sort, many possible subsidiary hy-

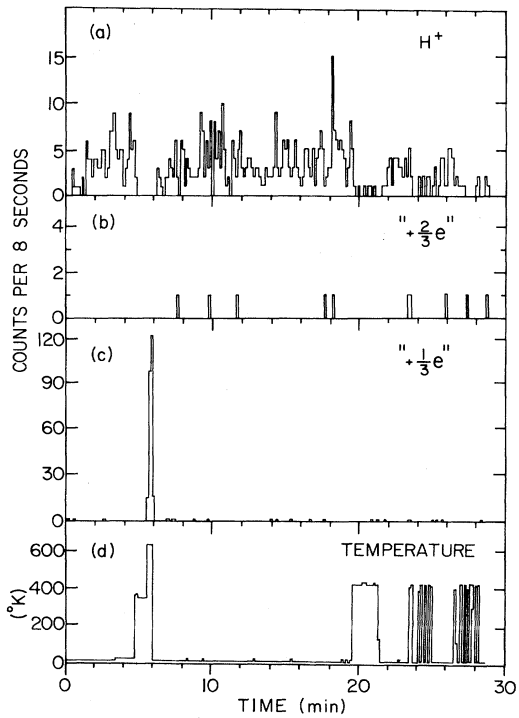

FIG. 24. Time distribution of events in three energy windows set on the spectrum of Fig. 23, from run F. The energy intervals for the windows were the same as in Fig. 5.

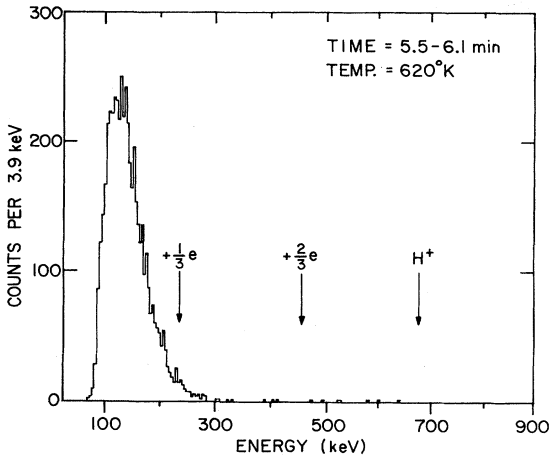

FIG. 25. Energy spectrum of particles recorded at an Nb temperature of 620 °K, from run F.

potheses. For instance, the assumption implicit in the hypothesis was that $(+\frac{1}{3}e)$ particles diffuse freely through solids of room temperature, just as hydrogen, or potassium ions diffuse through metals at $T \gg 1000$ °K. If these particles diffused through Nb more slowly, then they may be emitted over a period of days rather than seconds and may be lost in the background. Heating the Nb above room temperature to ~500 °K was intended to correct this defect—and this is also related to the negative results

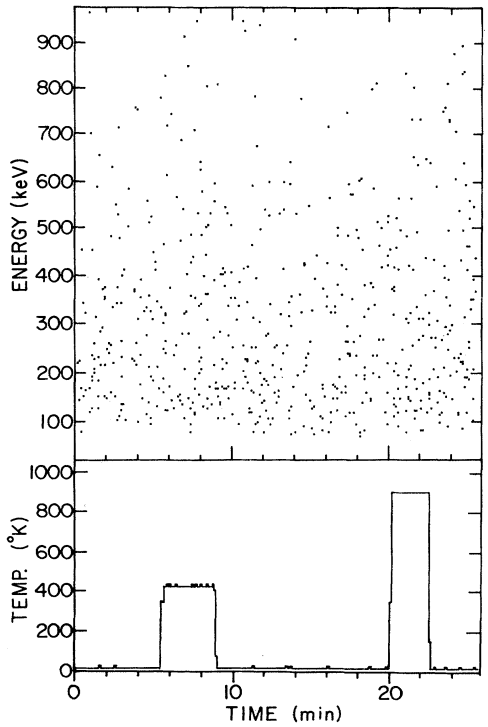

FIG. 26. Result of a search for light particles in run G, with He being leaked into the system and the thick Al absorber (4.8 mg/cm^2) in place.

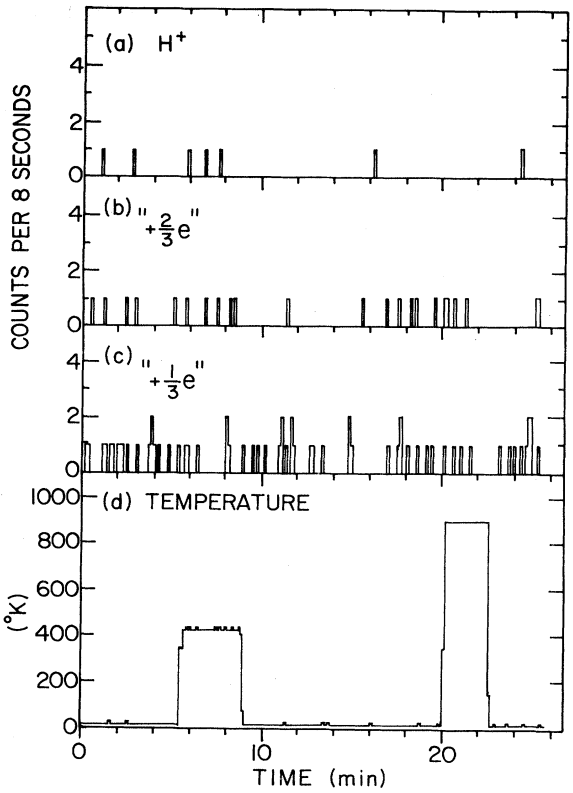

FIG. 27. Time distribution of events recorded in three energy windows set on the spectrum of Fig. 26, from run G. The energy intervals for the windows were the same as in Fig. 12.

from an earlier experiment[9] involving a Nb filament heated to 800 °K (but no cryogenic trapping). If fractional charges were trapped inside room temperature Nb, and low temperature played no special role, then the original hypothesis is certainly incorrect. Alternatively, the diffusion of fractional charges may be as postulated—with some exceptions. Thus there may be some materials in which fractional charges *are* trapped, or at least slowed down, even at room temperature. If some of the structural material in the vacuum housing, accelerator structure, or building were of this type, it would tend to shield the cold Nb from the postulated ambient "gas" of $(+\frac{1}{3}e)$ particles. Of course there were structural materials surrounding the Stanford experiment as well, and such effects are unlikely to have given complete (>99%) screening.

It is also conceivable that the purity (or surface purity) of the Nb plays some critical role in the trapping process. We have made no attempt at reproducing the type of surface treatment and annealing that was carried out for the Nb spheres in the Stanford measurement.

Clearly one could come up with a number of alternative explanations; negative results can hardly ever be conclusive. However, we think that our results rule out a class of possible explanations for the fractional charges observed by LaRue, Fairbank, Hebard, and Phillips.

TABLE I. Summary of results.

Run	Helium cooling[a] (hr)	Magnetic steerer (G)	Carbon stripper ($\mu g/cm^2$)	Electrostatic deflector (kV)	Aluminum absorber ($\mu g/cm^2$)	Silicon detector (μm)	Temperature (°K)	Δt (sec)	Counts[b] "$+\frac{1}{3}e$"	Counts[b] "$+\frac{2}{3}e$"	H^+
A	9.5	0	10	5	100	300	4.2	382	5	2	239
							350	29	0	0	5
							620	53	2	0	8
							280	56	0	0	12
							480	192	3	0	9
B	7.5	0	10	5	0	300	4.2	408	19	9	1726
							260	64	2	3	13
							450	88	3	2	11
							620	32	8	38	14
C	7.2	0	10	5	0	300	4.2	576	16	22	577
							220	112	4	1	13
							500	136	0	5	15
D	1.0	0	10	5	75	300	4.2	23040	572	120	8209
							Det.[c]	4320	36	3	1
E	9.7	2.0	10	0	4800	2000	4.2	296	10	3	2
							350	48	1	1	0
							500	48	0	0	0
							670	40	2	0	0
							800	40	2	0	1
F	1.5	0	10	5	100	300	4.2	120	1	0	60
							350	56	0	0	8
							620	32	249	0	0
							420	104	2	0	5
G	1.5	2.0	10	0	4800	2000	4.2	200	13	2	1
							420	200	6	5	3
							880	152	3	3	0

[a]Holding time at liquid helium temperature before data taking was started.
[b]Total number of counts in the respective energy and time windows. The position of the energy windows are those shown in the corresponding figures.
[c]Background of the detector, isolated from the accelerator [cf. Fig. 18(b)].

ACKNOWLEDGMENTS

We should like to thank C. M. Stevens for discussions on the source extraction system, J. R. Specht for technical help in setting up the experiment, and J. J. Napolitano for discussions on the paper. We acknowledge the generosity of the Fermilab management in supporting this experiment, at energies six orders of magnitude below the full capabilities of the facility. This research was supported by the U. S. Department of Energy under Contract W-31-109-Eng-38.

*Present address: The Hebrew University of Jerusalem, Jerusalem, Israel.

[1]L. W. Jones, Rev. Mod. Phys. 49, 717 (1977); C. L. Hodges, P. Abrams, A. R. Baden, R. W. Bland, D. C. Joyce, J. P. Royer, F. Wm. Walters, E. G. Wilson, P. G. Y. Wong, and K. C. Young, Phys. Rev. Lett. 47, 1651 (1981); M. Marinelli and G. Morpurgo, Phys. Rep. 85, 162 (1982); D. Liebowitz, M. Binder, and K. O. H. Ziock, Phys. Rev. Lett. 50, 1640 (1983).

[2]G. S. LaRue, W. M. Fairbank, and A. F. Hebard, Phys. Rev. Lett. 38, 1011 (1977); G. S. LaRue, W. M. Fairbank, and J. D. Phillips, *ibid.* 42, 142 (1979); G. S. LaRue, J. D. Phillips, and W. M. Fairbank, *ibid.* 46, 967 (1981).

[3]J. P. Schiffer, Phys. Rev. Lett. 48, 213 (1982).

[4]If one assumes that a cold Nb sphere (140 μm in radius) would trap fractionally charged particles, then for particles of $\sim\frac{1}{3}$ the proton mass with thermal velocities one needs one

particle/m^3 for the sphere to intercept one particle/hour; if one assumes the sphere to be shielded by other cooled metal surfaces over 99% of the solid angle, then this would correspond to intercepting about one particle/week.

[5]J. Lindhard, M. Scharff, and H. E. Schiøtt, K. Dan. Vidensk. Selsk. Mat. Fys. Medd. 33, 14 (1963).

[6]O. Heinz and R. T. Reaves, Rev. Sci. Instrum. 39, 1229 (1968).

[7]J. F. Ziegler, *Handbook of Stopping Cross-Sections for Energetic Ions in All Elements* (Pergamon, New York, 1980), Vol. 5.

[8]R. N. Boyd, S. L. Blatt, T. R. Donoghue, L. J. Dries, H. J. Hausman, and H. R. Suiter, Phys. Rev. Lett. 43, 1288 (1979).

[9]J. P. Schiffer, T. R. Renner, D. S. Gemmell, and F. P. Mooring, Phys. Rev. D 17, 2241 (1978).